



Remnants and Rates of Metamorphic Decarbonation in Continental Arcs

Evan J. Ramos*, Dept. of Geological Sciences, University of Texas, Austin, Texas 78712, USA; Jade Star Lackey, Geology Dept., Pomona College, Claremont, California 91711, USA; Jaime D. Barnes, Dept. of Geological Sciences, University of Texas, Austin, Texas 78712, USA; Anne A. Fulton**, Geology Dept., Pomona College, Claremont, California 91711, USA

ABSTRACT

Metamorphic decarbonation in magmatic arcs remains a challenge to impose in models of the geologic carbon cycle. Crustal reservoirs and metamorphic fluxes of carbon vary with depth in the crust, rock types and their stratigraphic succession, and through geologic time. When byproducts of metamorphic decarbonation (e.g., skarns) are exposed at Earth's surface, they reveal a record of reactive transport of carbon dioxide (CO₂). In this paper, we discuss the different modes of metamorphic decarbonation at multiple spatial and temporal scales and exemplify them through roof pendants of the Sierra Nevada batholith. We emphasize the utility of analogue models for metamorphic decarbonation to generate a range of decarbonation fluxes throughout the Cretaceous. Our model predicts that metamorphic CO, fluxes from continental arcs during the Cretaceous were at least 2 times greater than the present cumulative CO, flux from volcanoes, agreeing with previous estimates and further suggesting that metamorphic decarbonation was a principal driver of the Cretaceous hothouse climate. We lastly argue that our modeling framework can be used to quantify decarbonation fluxes throughout the Phanerozoic and thereby refine Earth systems models for paleoclimate reconstruction.

INTRODUCTION

How much "bark" was in the arc? The question of CO₂ contribution from magmatic arcs, especially continental arcs that poise platform carbonates in the paths of ascending magmas (Lee et al., 2013), is important given the power of tectonically outgassed CO₂ to modulate Earth's climate (e.g., Royer

et al., 2004; Lee et al., 2013; McKenzie et al., 2016). CO₂ fluxes from continental arcs are the cumulative expression of magmatism, contact metamorphism and assimilation of sedimentary rocks by magmas, and fluid flow through the crustal column. Because of its connection to magmatic and hydrothermal systems (e.g., Baumgartner and Ferry, 1991), metamorphic CO₂ production in continental arcs remains a challenge to quantify and has thus been on the periphery of most studies. The movement of CO, during metamorphism is further complicated by metamorphic reaction progress, fluid availability, geothermal gradients, and chemical potentials. Nonetheless, the strides made in studies of continental arcs position us to advance our understanding of metamorphic decarbonation through geologic time, its role in the carbon cycle, and its influence on past climates.

Maps of fossilized magmatic systems and experiments replicating sub-arc and lower crustal environments have been employed to estimate CO, fluxes from continental arcs. In general, these studies establish upper and lower estimates for CO, fluxes from continental arcs, but questions remain regarding the proportion of CO, produced via metamorphism. For example, estimates of area addition rates of magma through geologic time proxy for magma fluxes (Cao et al., 2017; Ratschbacher et al., 2019), which are critical parameters that set the tempo and duration of metamorphic decarbonation (e.g., Cathles et al., 1997). Without information regarding the rocks in which the magma intrudes, only magmatic CO, fluxes from continental arcs can be approximated. Experiments replicating sub-arc and lower crustal conditions show that carbonate rock can be almost wholly decarbonated (Carter and Dasgupta, 2016), which has been corroborated by observations of extremely low ¹³C/¹²C ratios of calc-silicate xenoliths from the Merapi volcano (Whitley et al., 2019). The degree to which continental arc magmas completely decarbonate their host rocks is unknown, but given the relatively open-system nature of continental arcs, these findings likely reflect upper limits for decarbonation rates.

The geochemical and isotopic composition of volcanic emissions from active continental arcs reveal CO₂ generated by metamorphism. A global compilation of CO₂/S_T measurements shows that arcs where magma intrudes platform carbonates often produce large CO₂ fluxes (Aiuppa et al., 2019). Moreover, the isotopic composition of volcanic emissions from these continental arcs further suggests input of sedimentary carbon (Mason et al., 2017). Despite these advancements, measurement uncertainty in these data hampers a quantitative assessment of the metamorphic proportion of continental arc CO₂ outputs. By focusing on active systems, this approach cannot convey how continental arc magmatism and concomitant CO, fluxes have changed through geologic time.

Numerical models have been useful in understanding metamorphism in continental arcs. Studies have typically scaled observations, such as changes in the length of continental arcs through time, to fluxes of metamorphic CO₂ (e.g., Mills et al., 2019; Wong et al., 2019). Although these methods provide meaningful boundary estimates, they do not fully consider the thermodynamics of reactive transport. Other studies have used

GSA Today, v. 30, https://doi.org/10.1130/GSATG432A.1. Copyright 2020, The Geological Society of America. CC-BY-NC.

^{*}Corresponding author: ejramos@utexas.edu.

^{**}Now at Dept. of Geology and Geological Engineering, Colorado School of Mines, Golden, Colorado 80401, USA.

numerical models of open-system heat and mass transfer (e.g., Nabelek et al., 2014; Chu et al., 2019), providing accurate flux estimates. The drawback of these models, however, is that they involve geologic specificity that belies a broad representation of metamorphism in continental arcs. To predict how metamorphic decarbonation has varied through geologic time, a balance between these common approaches needs to be found.

In this paper, we show that sedimentary, igneous, and metamorphic rock evidence can be used to quantify the rates of metamorphic decarbonation in continental arcs through the Phanerozoic. Metamorphic rocks in continental arcs can directly trace decarbonation rates, but the reactive transport processes involved in their formation is not simple. We thus review common rocks that form through metamorphic decarbonation in the shallow crust, the reactions and conditions that generate them, and the CO. amounts that they can release as a byproduct of their formation. Additionally, through numerical modeling, we demonstrate that the volume fraction of sedimentary rock that undergoes decarbonation can be related to the relative volumes of sedimentary rock and magma in continental arcs. This finding is validated against the well-characterized rock record of the Cretaceous Sierra Nevada batholith (SNB). When compiled stratigraphic sections of North America and arc magma fluxes through the Phanerozoic are imposed in our model, we predict how fluxes of CO, from metamorphic decarbonation changed through geologic time.

FIELD OBSERVATIONS OF DECARBONATION AND RE-CARBONATION IN THE ROCK RECORD

There is abundant rock-hosted evidence for CO, liberation, transport, and immobilization in exhumed arc crust within circum-Pacific batholiths, including the SNB. Whereas the isolated screens and roof pendants of metamorphic rocks appear as slivers in granitoid plutons, they are volumetrically underrepresented at Earth's surface due to erosion, overprinting by younger intrusions, and/or downward transport to the sub-arc during pluton emplacement (e.g., Ducea et al., 2015). These rocks show abundant evidence that carbonate-bearing rocks spanned from upper crustal contact aureoles to lower crustal granulite facies domains (e.g., Kerrick, 1977; Newberry and Einaudi, 1981). The capacities of these pendants to produce CO₂ are tied to their protoliths, fluid budgets, and reaction progresses (Fig. 1A).

Skarn rocks, composed of varying proportions of garnet, pyroxene \pm wollastonite, are synonymous with decarbonation (Fig. 1B) and are often associated with economic base and precious metal deposits. Skarns epitomize optimal conditions for releasing ${\rm CO_2}$ where infiltration of water-rich fluid main-

tains high chemical potentials, driving decarbonation locally to completion (e.g., Chu et al., 2019, and references therein). For example, a cubic meter of garnetite skarn signifies 1.01-1.05 metric tons of CO_2 released from calcite (Lee and Lackey, 2015).

Skarns often form at shallow crustal depths (3–5 km) and along the margins of granitoid rocks that intruded into carbonates.

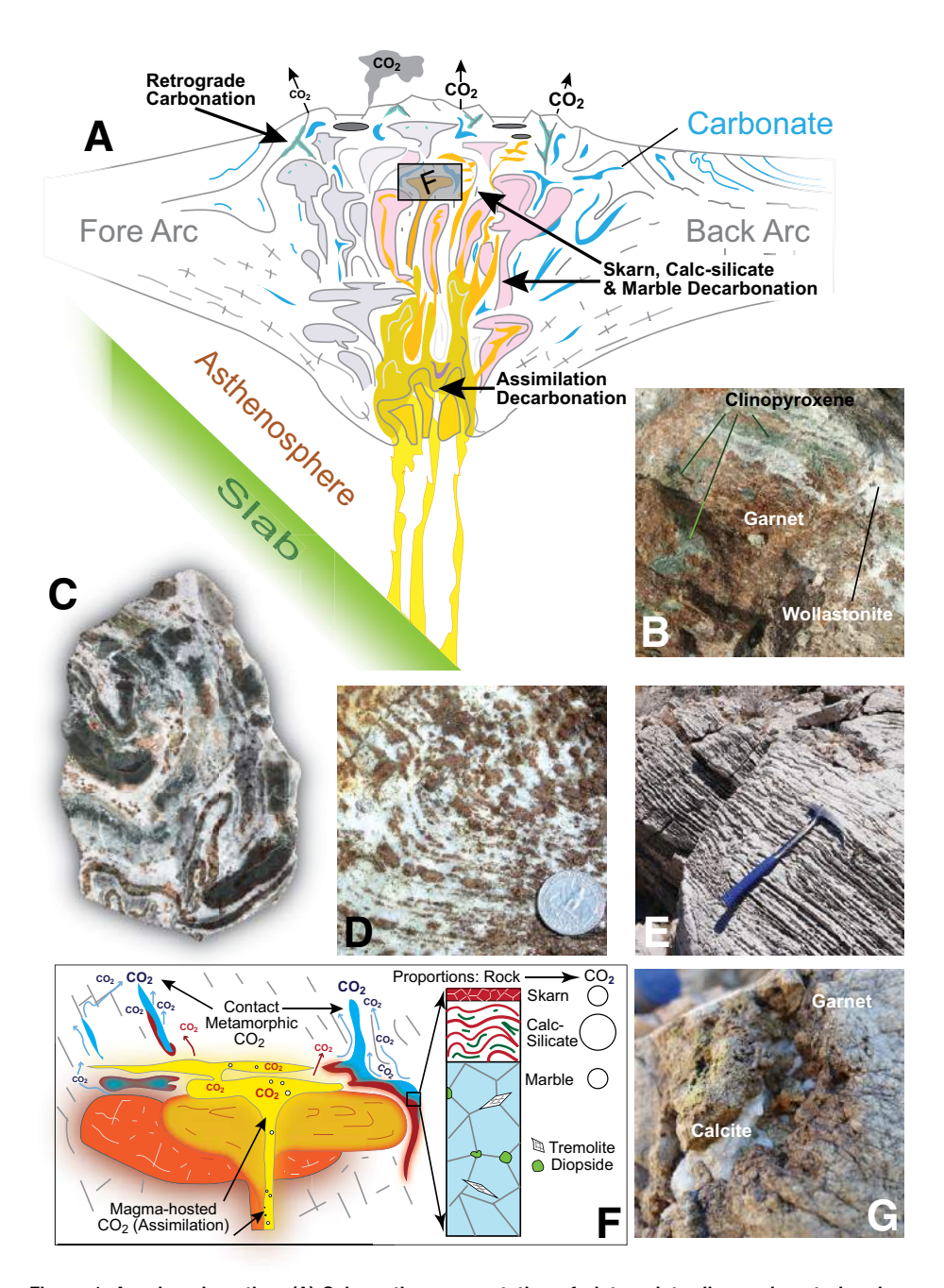


Figure 1. Arc decarbonation. (A) Schematic representation of plutons intruding carbonate-bearing crust at various depths in a magmatic arc (not to scale); (B) 30-cm-wide outcrop of garnet, clinopyroxene, and wollastonite (white) typical of Sierra Nevada batholith skarn; (C) 20-cm-wide slab of garnet-wollastonite-diopside calc-silicate rock with folding of original sedimentary structures; (D) calc-silicate with garnet (red) showing traces of Al-rich domains in garnet-wollastonite calc-silicate (coin is 24 mm across); (E) laminated carbonate typical of rocks metamorphosed to form C and D (hammer is 28 cm long); (F) cartoon depicting metamorphic decarbonation, common metamorphic rock types, their protoliths, CO₂ yields; (G) retrograde calcite deposited in 1-cm-wide cavity within garnet skarn.

Any carbonate that was not converted to skarn coarsens into *marble*. Marbles are more abundant than skarns (Fig. 2B) and can appear to be relatively unaffected by metamorphic decarbonation. Yet, small amounts of reaction progress are enabled by trace quantities (<5 modal %) of quartz present, producing considerable amounts of CO₂ (~32–46 kg CO₂ per cubic meter of rock; Ferry, 1989). Further, if marble bodies abut

water-rich metapelitic units, CO₂ can diffuse out of the marble and thus export nontrivial amounts of CO₂ (e.g., Vidale and Hewitt, 1973; Ague, 2000).

Calc-silicate rocks, with white, green, or red laminations inherited from sedimentary laminations, are also composed of microcrystalline wollastonite, pyroxene, and garnet (Fig. 1C–1E). Whereas skarns see copious CO₂ release by fluid infiltration and

metasomatism of originally pure carbonate rocks, calc-silicates release similar amounts of CO₂ because interbedded layers of carbonate, silica, and clay minerals predispose mixed carbonate-siliciclastic rocks to fully decarbonate (Fig. 1F). Water-rich fluids are still necessary to fully decarbonate these rocks, but their laminated character can cause a positive feedback that enables near-complete decarbonation. The enhancement of permeability during decarbonation promotes CO₂ transport, enabling further decarbonation (e.g., Zhang et al., 2000).

Even if thermodynamic conditions enable

Even if thermodynamic conditions enable decarbonation to proceed, not all CO, produced makes it out of the crust. CO, is most often immobilized when low crustal permeability inhibits fluid flow or magma production rates decrease. Secondary carbonate deposition represents CO, immobilization in arcs, often occurring away from hotter, deeper areas of the arc crust, and down temperature gradients. Examples include calcite veins that cross-cut skarn rocks and precipitate in vugs and brittle fractures (Fig. 1G). Other silicates that form when CO, is mineralized, including retrograde serpentine and tremolite, occur appreciably (up to 2 wt%), even when crustal permeability is high enough to promote continued CO, removal (Nabelek et al., 2014). Veins and deposits at shallower levels in the crust are further evidence that CO₂ can be reprecipitated. Even granitoids in arc crust are noted to contain regular but small amounts of calcite (0.2–1.0 wt%; White et al., 2005). Overall, these observations suggest that seemingly trace amounts of retrograde CO, mineralization can manifest in large masses of CO, left behind after prograde metamorphic decarbonation.

The journey of an individual molecule of CO₂ can be complicated by a series of prograde and retrograde reactions at different times and locations in the arc crust. Yet, at a fundamental level, the amount of metamorphically derived CO₂ that exits from continental arcs directly relates to the composition of rocks that comprise the arc and the amount of magma that is emplaced over a given time. These underlying principles, while still considering the intricacies of metamorphic decarbonation and its geologic record, motivate our model design.

ANALOGUE MODEL FOR METAMORPHIC DECARBONATION

The basis of the analogue model is to determine the volume of sedimentary rock

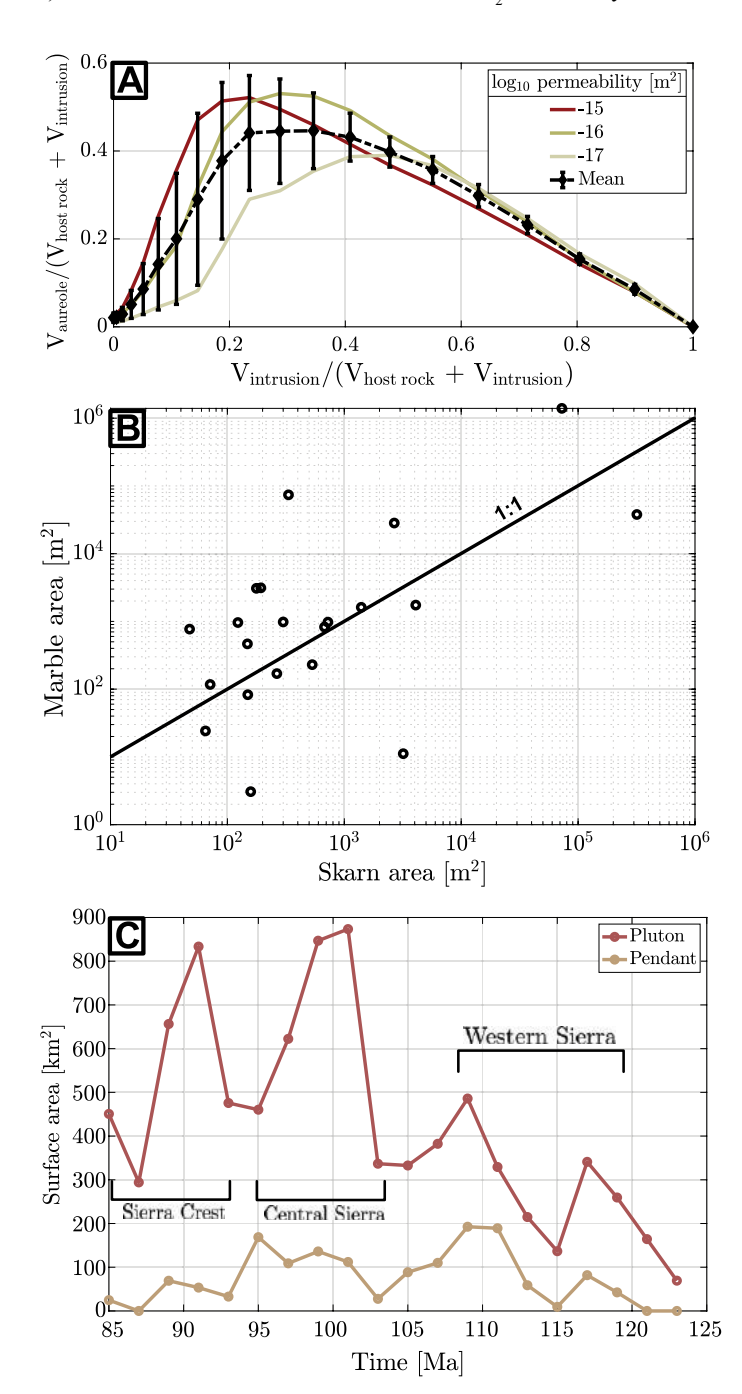


Figure 2. (A) Predicted volume fraction of aureole as a function of volume fraction of intrusion. Error is 1σ . (B) Skarn-marble area distributions for a corridor of the Sierra Nevada batholith (SNB). (C) Surface area addition rates for intrusions and metamorphic pendants in the SNB through the 40 m.y. of elevated magmatic activity.

that undergoes decarbonation in a continental arc. The model simulates two-dimensional fluid flow, heat transfer, and fluidrock oxygen isotope exchange after the emplacement of an intrusion as a proxy for metamorphic decarbonation (further model setup and assumptions are described in Ramos et al., 2018, and in the Supplementary Information¹). The δ^{18} O values of carbonates decrease during progressive decarbonation (e.g., Bowman, 1998). Therefore, in each simulation, we track the changes in host-rock δ¹⁸O values during hydrothermal fluid flow to highlight areas around a magma body that meet likely conditions for decarbonation. Once hydrothermal activity has ceased, the δ^{18} O values of the host rock define a volume of rock that undergoes decarbonation, which we term the aureole volume.

Our numerical model considers effects of crustal permeability and magma volume on aureole volumes. The model domain remains constant across each simulation (i.e., $V_{host rock}$ + $V_{intrusion}$ = constant; Fig. DR3, see footnote 1). A series of model runs predicts aureole volumes as a function of intrusion volume and crustal permeability where the largest volumes of decarbonated host rock $(V_{aureole})$ are at intermediate relative intrusion volumes (Fig. 2A). Effectively, as magma volumes exceed the volume of host rock in an arc, the aureole volume diminishes, concomitant to a diminished aureole decarbonation flux. This result counters common thought, where continental arc flare-ups (i.e., times of maximum intrusion volume) are thought to be times of maximum CO₂ output from arcs (Lee and Lackey, 2015).

The mineralogy of the host rocks in which the magma intrudes controls the magnitude of the decarbonation flux it produces. We thus amass magma addition rates and sedimentary rock information—including rock types, depositional ages, and stratigraphic thicknesses-for the SNB and the entirety of North America. Details about how we compare sedimentary and magma volumes through time are given in the Supplementary Information, but in short, our model predicts a metamorphic CO, flux—which includes CO, produced via metamorphism in the aureole and by assimilation of host rock in the intrusion—based off this volume comparison. Independent of the model, we compute a CO, flux for the Cretaceous SNB by scaling the area distribution of metamorphic

pendants and skarns within a portion of the SNB to amounts of produced CO₂ along the entire arc. This estimate is compared to our model prediction to assess its utility in estimating CO₂ fluxes.

GROUND-TRUTHING THE ANALOGUE MODEL WITH THE GEOLOGIC RECORD FROM THE CRETACEOUS SNB

The area distribution of skarns (Fig. 2B) varies considerably along the SNB corridor we examined, with some exposures containing <10 m² of skarn and others containing >1 km². The skarn area is generally dwarfed by the marble area and only comprises 4% of the total mapped area. If we assume a maintained skarn-marble ratio within pendants along the entire SNB, an average carbonate fraction in sedimentary rocks in the arc of 20%, and skarn occurrence over 7 km of depth in the SNB, we compute a total skarn volume in the SNB of 19,000 km3. This volume, if decarbonated over a 40 m.y. time interval, produces an average CO₂ flux of ~1 Mt/yr. This value, which excludes CO₂ from calc-silicates and marbles and fluxes from magma degassing and assimilation, is fivefold less than measurements of modern global continental arcs that intersect platform carbonates (5 Mt/yr; Aiuppa et al., 2019) and nearly two orders of magnitude less than previous estimates for net CO, fluxes from all Cretaceous continental arcs (Lee et al., 2013; Lee and Lackey, 2015). This disparity can largely be attributed to the sparse distribution of metamorphic pendants in the SNB and the difficulty of computing assimilation fluxes from the geologic record. Thus, this skarn CO, flux is considered a minimum estimate for metamorphic CO, fluxes from the Cretaceous SNB.

When sedimentary rock volumes and proportions from SNB-specific sites (Fig. DR2, see footnote 1) are compared with granitoid volumes emplaced in North America from 125 to 85 Ma (Cao et al., 2017), we predict the net metamorphic CO₂ flux from North American arcs to be 32.3 ± 28.4 Mt/yr during the Cretaceous, with 13% of the flux deriving from assimilated wall rock and 87% coming from decarbonation in the aureole (see Supplementary Information for further details on the flux calculation). Western SNB rocks, typified by the Triassic–Jurassic Kings Sequence (Fig. DR2), which contains

both mixed carbonate-siliciclastic rocks and platform carbonates, contribute 59% of all generated CO₂. Paleozoic sections such as the Morrison block in the eastern SNB, which are composed predominantly of siliciclastic rocks and 23% carbonate, contribute 41%. Notably, this net flux agrees within 2σ error of the net decarbonation estimate from (1) SNB skarn outcrops (1 Mt/yr) and when (2) North American sedimentary rock information is used (40 Mt/yr) instead of SNBspecific stratigraphic sections (Fig. 3C at ca. 100 Ma time marker). Although locationspecific geology will always yield more accurate flux estimates, these findings support the utility of North American sedimentary rocks as a globally representative archive of sedimentary rock types.

PHANEROZOIC METAMORPHIC DECARBONATION RATES

The variational growth rate of sedimentary rock and granitoid volumes underpins the changes in decarbonation rates in continental arcs through time (negative slope of lines in Fig. 3A). Once corrected for erosion (assuming an erosional half-life of 400 m.y. sensu Cao et al., 2017), sedimentary rocks from North America, granitoids (from Cao et al., 2017), and their volumetric distributions grow unsteadily. Cambrian through Devonian time (542-400 Ma) is marked by similar rates of growth of different rock types, highlighting the voluminous deposition of carbonate throughout the Phanerozoic. The volume of mixed carbonate-siliciclastic rocks surpasses that of pure carbonate by latest Pennsylvanian (ca. 300 Ma) when the growth rate of siliciclastic rocks increases well beyond all other rock types. Sediment deposition rates plateau in the Triassic (245-206 Ma) after the assembly of Pangea (Cao et al., 2017) and subsequently increase upon its breakup in the Jurassic (ca. 180 Ma). Carbonate and mixed carbonate-siliciclastic rocks grow in volume in the Cretaceous but are dwarfed by increases in the siliciclastic deposition rate. These trajectories of growth remain constant through the Cenozoic.

Change in area addition rates of granitoid is out of phase with the deposition of sedimentary rocks (Fig. 3A). Globally, granitoid volumes grow at a roughly consistent rate until the breakup of Pangea, whereupon their cumulative volumes grow rapidly. Continental arc activity in North America is quiescent

GSA Data Repository item 2020150, including model descriptions and data sources for rock type information, is available online at https://www.geosociety.org/datarepository/2020.

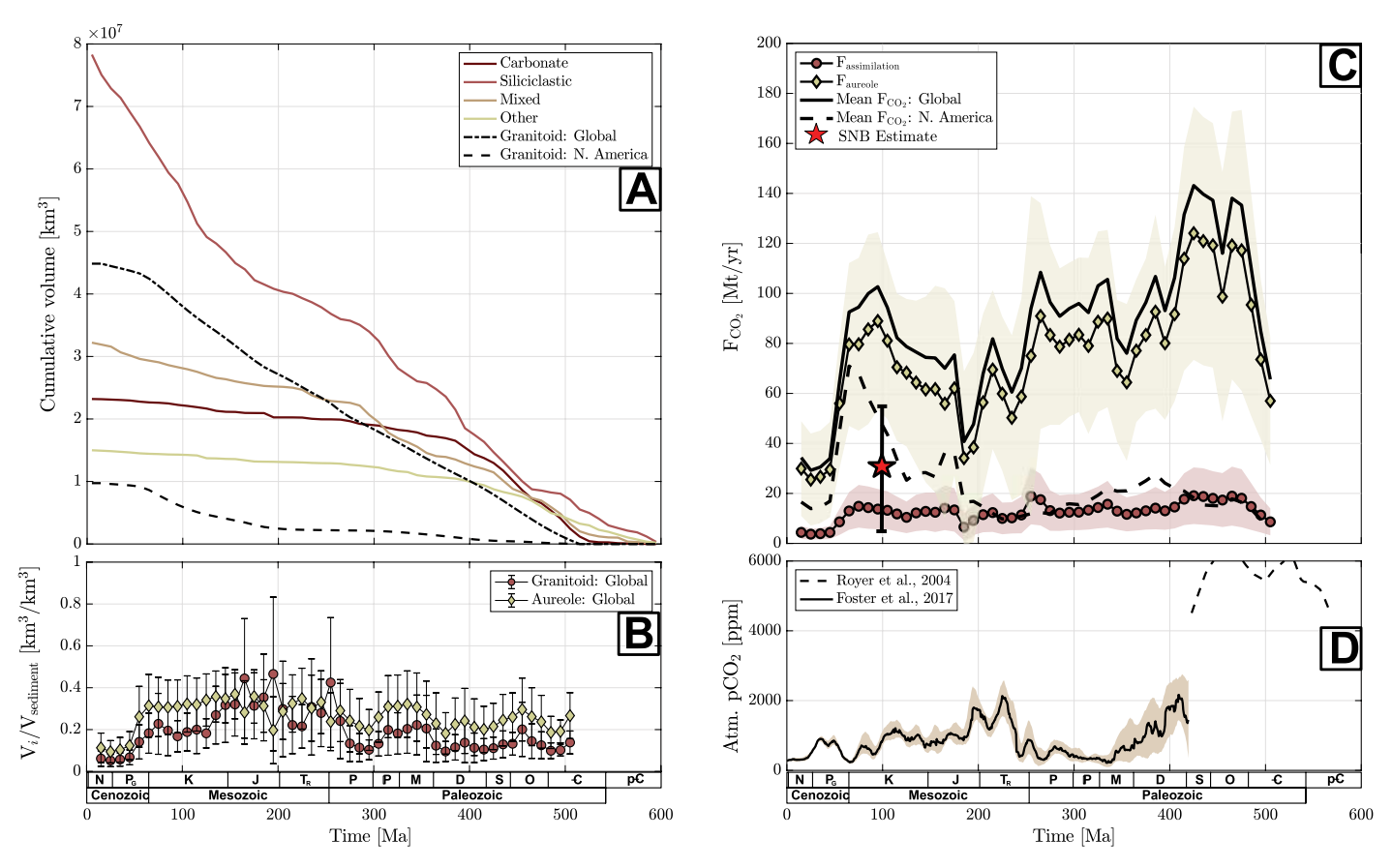


Figure 3. Phanerozoic estimates of rock volumes and decarbonation fluxes. All errors are 1 standard deviation (error bars in B and shaded volumes in C and D). (A) Cumulative volume estimates for all rock types. Rates of deposition (in units of volume/time) can be gleaned by the negative slope of the lines. (B) Volume fractions of intrusions and aureoles. (C) Metamorphic decarbonation fluxes, including the Sierra Nevada batholith (SNB)-specific flux. (D) Atmospheric pCO₂ estimates from the GEOCARB model from 570 to 420 Ma (Royer et al., 2004) and from measurements 420 Ma-present (Foster et al., 2017).

through much of the Paleozoic but quickly grows throughout the Mesozoic, punctuated by volumetrically significant emplacement of granitoids and coinciding with the formation of the large metamorphic pendants of the SNB. Juxtaposing increases in sediment deposition rates in the Cenozoic, area addition rates of granitoid decrease by threefold (fig. 4C *in* Cao et al., 2017).

Changes in the size of igneous and sedimentary rock volumes manifest in changes in metamorphic decarbonation rates through time, where gradual decreases in F_{CO_2} are predicted from the Cambrian toward the present (Fig. 3C). The confluence of high granitoid area addition rates and high proportions of carbonate rocks produces the highest metamorphic decarbonation fluxes, between the Cambrian and Silurian (540-420 Ma), where fluxes oscillate between 120 and 140 Mt/yr, or almost 2-3 times the current flux of CO, from all volcanoes (Fischer et al., 2019). This maximum net CO, flux contrasts with the minima in the Cenozoic (66-5 Ma), where granitoid area addition rates decrease by threefold, and <20% of all sediments undergo decarbonation (Fig. 3B).

Decarbonation within the aureole produces significantly more CO₂ than from assimilation of host rock by the emplaced magma, even when the volume fraction of the granitoid exceeds that of the aureole (Fig. 3B). Less decarbonation is predicted when the volume fraction of granitoids is highest (225 and 180 Ma). This marked decrease in net decarbonation fluxes underscores the propensity for metasomatized sedimentary rocks to produce more CO₂ than their assimilated counterparts. Nonetheless, all assimilated CO₂ fluxes are appreciable and within error of previous degassing estimates (Ratschbacher et al., 2019).

METAMORPHIC DECARBONATION IN THE GEOLOGIC CARBON CYCLE

The simplest way to assess the role of metamorphic decarbonation at continental arcs in the geologic carbon cycle is to compare its magnitude to those of other "endogenic" CO₂ fluxes, which are fluxes from the solid Earth (endogenic system) to the hydrosphere, biosphere, and atmosphere (exogenic system). From our model, the range of global metamorphic CO₂ fluxes we predict through the

Phanerozoic (27–129 Mt/yr; Fig. 3C) is similar in magnitude to all other endogenic CO₂ fluxes (Table 1). The similarity in the range of the fluxes underscores the likelihood of the geologic carbon cycle maintaining an equilibrium state over million-year timescales (Berner and Caldeira, 1997). Endogenic CO₂ fluxes should change, however, as paleogeography, hypsometry, sea level, and the thermal states of Earth's crust and mantle change (e.g., Kelemen and Manning, 2015; Lee et al., 2018). How endogenic CO₂ fluxes temporally change, concomitant with other changes in the Earth system, remains an open question.

As an integrative climate metric, atmospheric pCO_2 is influenced by all fluxes of CO_2 between the atmosphere and solid Earth, which makes it challenging to determine the dominant CO_2 fluxes through geologic time. While endogenic fluxes establish base-level climate states, atmospheric pCO_2 is also influenced by silicate weathering, organic carbon burial, oxidation of organic matter, and the paleogeography of crustal material (e.g., Kump et al., 2000; Macdonald et al., 2019). Most tectonic

TABLE 1. COMPARISON AND SUMMARY OF ESTIMATES OF ENDOGENIC CO., FLUXES

Flux type	Magnitude (Mt/yr)	Method(s) for estimation	Reference(s)
Cretaceous continental arcs (Sierra Nevada batholith)	1	Area distribution of skarn	This study
Cretaceous continental arcs (North America)	4–58	Analogue decarbonation model with Sierra Nevada batholith stratigraphy	This study
Cretaceous continental arcs (global)	85–127	Mass balance calculation	Lee et al. (2013)
Contact metamorphism in continental arcs (global)	0.7–11	Reactive transport model	Chu et al. (2019)
Mid-ocean ridges (global)	53–97	^a Geochemical analysis of mid-ocean ridge basalt glasses; ^b measurement of noble gas fluxes at mid-ocean ridges; ^c geochemical analyses of emitted volatiles from mid-ocean ridges; ^d petrologic analysis of basaltic magmas	^a Marty and Tolstikhin (1998) ^b Hilton et al. (2002) ^c Fischer (2008) ^d Dasgupta and Hirschmann (2010)
Continental rifts	4	Gas efflux measurements	Lee et al. (2016)
Mountain building	13–440	^a Petrologic and geochemical measurements of exhumed metamorphic rocks; ^b geochemical analysis of groundwater draining active mountain belt; ^c geochemical analyses of hydrothermal fluids in active mountain belts; ^d thermodynamic modeling (<i>P-T-t</i> path calculations) of exhumed metamorphic rocks	^a Kerrick and Caldeira (1998) ^a Skelton (2011) ^b Chiodini et al. (2000) ^c Becker et al. (2008) ^d Stewart and Ague (2018)

fluxes appear weakly correlated with $p\text{CO}_2$ from 200 Ma to present (Wong et al., 2019). From our predictions, we find that the connection between metamorphic CO_2 fluxes from continental arcs and atmospheric $p\text{CO}_2$ is tenuous (Fig. 3D). Beyond the similar decreases from the Cambrian toward the present and the shared relative maxima prior to the Devonian, atmospheric $p\text{CO}_2$ and metamorphic CO_2 fluxes appear disconnected and cannot be wholly compared without knowledge of other fluxes.

Nonetheless, times where the correlation between metamorphic CO, fluxes and atmospheric pCO_2 are weakest can be leveraged to explore the operation of other Earth system processes. For example, between 320 and 270 Ma during icehouse conditions in the Permian, metamorphic CO, fluxes remain high while atmospheric pCO_2 is low. This time interval also coincides with the waning stages of Pangea formation. Despite elevated metamorphic fluxes, could atmospheric pCO_2 have remained low because generation of relief during supercontinent assembly enhanced silicate weathering (e.g., West et al., 2005)? Instead, could there have been prolonged organic carbon burial as equatorial regions remained hot and humid and forests proliferated (Ronov, 1982)? For a contrasting example, in Permian-Triassic time after Pangea's assembly, atmospheric pCO_{2} increases while metamorphic CO_{2} fluxes drop by a factor of 2. Does atmospheric pCO₂ increase because the aridification of continental interiors inhibits silicate weathering? If so, can modest CO₂ outputs from continental arcs with diminished silicate weathering fluxes be enough to increase atmospheric pCO_2 by a factor of 2, or are

other endogenic fluxes necessary, such as organic carbon oxidation or continental rifting (e.g., Lee et al., 2016)? Between these contrasting scenarios, the unifying question concerns the thresholds at which metamorphic CO_2 fluxes can be attributed to the development of past climates, if at all.

Of all time periods on Earth, the Cretaceous period likely represents a time in which enhanced continental arc metamorphism promoted a hothouse climate. The emergence of deep-water calcifiers in the Triassic (e.g., Ridgwell and Zeebe, 2005), increases in granitoid addition rates, doubling in length of continental arcs that intersect crustal carbonates (Lee et al., 2013), and increased evidence of skarn formation within circum-Pacific batholiths (e.g., Lee and Lackey, 2015) support the plausibility of elevated metamorphic CO, fluxes contributing to hothouse climate conditions in the Cretaceous. Our model predicts maximum values for aureole volume fractions during the Mesozoic (Fig. 3B), purporting an increased proportion of aureole decarbonation. The average metamorphic CO, flux from arcs during the Cretaceous exceeds estimates for mid-ocean ridge CO, fluxes (60 Mt/yr; Wong et al., 2019). Unless CO, fluxes from continental rifts or oxidation of organic matter were significant in magnitude during the Cretaceous, continental arc metamorphism likely contributed the largest fraction of CO, of all endogenic fluxes. With further quantifications of endogenic CO, fluxes and their variation through time, benchmarked against known climatic changes, the role of tectonic outgassing in the evolution of Earth's climate will become increasingly clear.

ACKNOWLEDGMENTS

J. Muller and J. Ryan-Davis helped with digitizing maps for area calculations. We thank C.-T.A. Lee for comments on an early draft of the paper, two anonymous reviewers for thorough suggestions, and M. Ducea for careful editorial handling. All MATLAB codes used in the analogue model and for figure generation can be found in the GitHub repositories of the first author: https://github.com/ejramos/Phanerozoic_decarbonation. National Science Foundation grant NSF-OCE-1338842 awarded to Lackey, Barnes, and others as part of the Frontiers in Earth Systems Dynamics program supported this work.

REFERENCES CITED

Ague, J.J., 2000, Release of CO₂ from carbonate rocks during regional metamorphism of lithologically heterogeneous crust: Geology, v. 28, no. 12, p. 1123–1126, https://doi.org/10.1130/0091-7613(2000)28<1123:ROCFCR>2.0.CO;2.

Aiuppa, A., Fischer, T.P., Plank, T., and Bani, P., 2019, CO₂ flux emissions from the Earth's most actively degassing volcanoes, 2005–2015: Scientific Reports, v. 9, no. 1, article no. 5442, https://doi.org/10.1038/s41598-019-41901-y.

Baumgartner, L.P., and Ferry, J.M., 1991, A model for coupled fluid-flow and mixed-volatile mineral reactions with applications to regional metamorphism: Contributions to Mineralogy and Petrology, v. 106, no. 3, p. 273–285, https://doi.org/10.1007/BF00324557.

Becker, J.A., Bickle, M.J., Galy, A., and Holland, T.J., 2008, Himalayan metamorphic CO₂ fluxes: Quantitative constraints from hydrothermal springs: Earth and Planetary Science Letters, v. 265, no. 3–4, p. 616–629, https://doi.org/ 10.1016/j.epsl.2007.10.046.

Berner, R.A., and Caldeira, K., 1997, The need for mass balance and feedback in the geochemical carbon cycle: Geology, v. 25, no. 10, p. 955–956, https://doi.org/10.1130/0091-7613(1997)025<0955: TNFMBA>2.3.CO;2.

Bowman, J.R., 1998, Stable-isotope systematics of skarns, in Lentz, D.R., ed., Mineralized intrusion-related skarn systems: Quebec, Mineralogical Association of Canada, Short Course Series, v. 26, p. 99–145.

- Cao, W., Lee, C.T.A., and Lackey, J.S., 2017, Episodic nature of continental arc activity since 750 Ma: A global compilation: Earth and Planetary Science Letters, v. 461, p. 85–95, https://doi.org/10.1016/j.epsl.2016.12.044.
- Carter, L.B., and Dasgupta, R., 2016, Effect of melt composition on crustal carbonate assimilation: Implications for the transition from calcite consumption to skarnification and associated CO₂ degassing: Geochemistry, Geophysics, Geosystems, v. 17, no. 10, p. 3893–3916, https://doi.org/ 10.1002/2016GC006444.
- Cathles, L.M., Erendi, A.H.J., and Barrie, T., 1997, How long can a hydrothermal system be sustained by a single intrusive event?: Economic Geology, v. 92, no. 7–8, p. 766–771, https://doi.org/10.2113/gsecongeo.92.7-8.766.
- Chiodini, G., Frondini, F., Cardellini, C., Parello, F., and Peruzzi, L., 2000, Rate of diffuse carbon dioxide Earth degassing estimated from carbon balance of regional aquifers: The case of central Apennine, Italy: Journal of Geophysical Research. Solid Earth, v. 105, no. B4, p. 8423–8434, https://doi.org/10.1029/1999JB900355.
- Chu, X., Lee, C.T.-A., Dasgupta, R., and Cao, W., 2019, The contribution to exogenic CO₂ by contact metamorphism at continental arcs: A coupled model of fluid flux and metamorphic decarbonation: American Journal of Science, v. 319, no. 8, p. 631–657, https://doi.org/10.2475/08.2019.01.
- Dasgupta, R., and Hirschmann, M.M., 2010, The deep carbon cycle and melting in Earth's interior: Earth and Planetary Science Letters, v. 298, no. 1–2, p. 1–13, https://doi.org/10.1016/j.epsl.2010.06.039.
- Ducea, M.N., Saleeby, J.B., and Bergantz, G., 2015, The architecture, chemistry, and evolution of continental magmatic arcs: Annual Review of Earth and Planetary Sciences, v. 43, p. 299–331, https://doi.org/10.1146/annurev-earth-060614-105049.
- Ferry, J.M., 1989, Contact metamorphism of roof pendants at Hope Valley, Alpine County, California, USA: Contributions to Mineralogy and Petrology, v. 101, no. 4, p. 402–417, https://doi.org/10.1007/BF00372214.
- Fischer, T.P., 2008, Fluxes of volatiles (H₂O, CO₂, N₂, Cl, F) from arc volcanoes: Geochemical Journal, v. 42, p. 21–38, https://doi.org/10.2343/geochemj.42.21.
- Fischer, T.P., Arellano, S., Carn, S., Aiuppa, A., Galle, B., Allard, P., Lopez, T., Shinohara, H., Kelly, P., Werner, C., and Cardellini, C., 2019, The emissions of CO₂ and other volatiles from the world's subaerial volcanoes: Scientific Reports, v. 9, no. 1, p. 1–11, https://doi.org/10.1038/s41598-019-54682-1.
- Foster, G.L., Royer, D.L., and Lunt, D.J., 2017, Future climate forcing potentially without precedent in the last 420 million years: Nature Communications, v. 8, article no. 14845, https://doi.org/10.1038/ncomms14845.
- Hilton, D.R., Fischer, T.P., and Marty, B., 2002, Noble gases and volatile recycling at subduction zones: Reviews in Mineralogy and Geochemistry, v. 47, no. 1, p. 319–370, https://doi.org/10.2138/rmg.2002.47.9.
- Kelemen, P.B., and Manning, C.E., 2015, Reevaluating carbon fluxes in subduction zones, what goes down, mostly comes up: Proceedings of the National Academy of Sciences of the United States of America, v. 112, no. 30, p. E3997–E4006, https://doi.org/10.1073/pnas.1507889112.
- Kerrick, D.M., 1977, The genesis of zoned skarns in the Sierra Nevada, California: Journal of Petrolo-

- gy, v. 18, no. 1, p. 144–181, https://doi.org/10.1093/petrology/18.1.144.
- Kerrick, D.M., and Caldeira, K., 1998, Metamorphic CO₂ degassing from orogenic belts: Chemical Geology, v. 145, no. 3–4, p. 213–232, https://doi.org/10.1016/S0009-2541(97)00144-7.
- Kump, L.R., Brantley, S.L., and Arthur, M.A., 2000, Chemical weathering, atmospheric CO₂, and climate: Annual Review of Earth and Planetary Sciences, v. 28, no. 1, p. 611–667, https:// doi.org/10.1146/annurev.earth.28.1.611.
- Lee, C.T.A., and Lackey, J.S., 2015, Global continental arc flare-ups and their relation to long-term greenhouse conditions: Elements, v. 11, no. 2, p. 125–130, https://doi.org/10.2113/gselements.11.2.125.
- Lee, C.T.A., Shen, B., Slotnick, B.S., Liao, K., Dickens, G.R., Yokoyama, Y., Lenardic, A., Dasgupta, R., Jellinek, M., Lackey, J.S., and Schneider, T., 2013, Continental arc-island arc fluctuations, growth of crustal carbonates, and long-term climate change: Geosphere, v. 9, no. 1, p. 21–36, https://doi.org/10.1130/GES00822.1.
- Lee, C.T.A., Caves, J., Jiang, H., Cao, W., Lenardic, A., McKenzie, N.R., Shorttle, O., Yin, Q.Z., and Dyer, B., 2018, Deep mantle roots and continental emergence: Implications for whole-Earth elemental cycling, long-term climate, and the Cambrian explosion: International Geology Review, v. 60, no. 4, p. 431–448, https://doi.org/10.1080/00206814.2017.1340853.
- Lee, H., Muirhead, J.D., Fischer, T., Ebinger, C.J., Kattenhorn, S., and Kianji, G., 2016, Tectonic degassing of mantle-derived CO₂ along faults in the East African Rift: Nature Geoscience, v. 9, no. 2, p. 145–149, https://doi.org/10.1038/ngeo2622.
- Macdonald, F.A., Swanson-Hysell, N.L., Park, Y., Lisiecki, L., and Jagoutz, O., 2019, Arc-continent collisions in the tropics set Earth's climate state: Science, v. 364, no. 6436, p. 181–184, https://doi .org/10.1126/science.aav5300.
- Marty, B., and Tolstikhin, I.N., 1998, CO₂ fluxes from mid-ocean ridges, arcs and plumes: Chemical Geology, v. 145, no. 3–4, p. 233–248, https://doi.org/10.1016/S0009-2541(97)00145-9.
- Mason, E., Edmonds, M., and Turchyn, A.V., 2017, Remobilization of crustal carbon may dominate volcanic arc emissions: Science, v. 357, no. 6348, p. 290–294, https://doi.org/10.1126/science.aan5049.
- McKenzie, N.R., Horton, B.K., Loomis, S.E., Stockli, D.F., Planavsky, N.J., and Lee, C.T.A., 2016, Continental arc volcanism as the principal driver of icehouse-greenhouse variability: Science, v. 352, no. 6284, p. 444–447, https://doi.org/10.1126/science.aad5787.
- Mills, B.J., Krause, A.J., Scotese, C.R., Hill, D.J., Shields, G.A., and Lenton, T.M., 2019, Modelling the long-term carbon cycle, atmospheric CO₂, and Earth surface temperature from late Neoproterozoic to present day: Gondwana Research, v. 67, p. 172–186, https://doi.org/10.1016/j.gr.2018.12.001.
- Nabelek, P.I., Bédard, J.H., and Rainbird, R.H., 2014, Numerical constraints on degassing of metamorphic CO₂ during the Neoproterozoic Franklin large igneous event, Arctic Canada: Geological Society of America Bulletin, v. 126, p. 759–772, https://doi.org/10.1130/B30981.1.
- Newberry, R.J., and Einaudi, M.T., 1981, Tectonic and geochemical setting of tungsten skarn mineralization in the Cordillera: Arizona Geological Society Digest, v. 14, p. 99–111.
- Ramos, E.J., Hesse, M.A., Barnes, J.D., Jordan, J.S., and Lackey, J.S., 2018, Reevaluating fluid sources during

- skarn formation: An assessment of the Empire Mountain skarn, Sierra Nevada, USA: Geochemistry, Geophysics, Geosystems, v. 19, no. 10, p. 3657–3672, https://doi.org/10.1029/2018GC007611.
- Ratschbacher, B.C., Paterson, S.R., and Fischer, T.P., 2019, Spatial and depth-dependent variations in magma volume addition and addition rates to continental arcs: Application to global CO₂ fluxes since 750 Ma: Geochemistry, Geophysics, Geosystems, v. 20, p. 2997–3018, https://doi.org/10.1029/2018GC008031.
- Ridgwell, A., and Zeebe, R.E., 2005, The role of the global carbonate cycle in the regulation and evolution of the Earth system: Earth and Planetary Science Letters, v. 234, no. 3–4, p. 299–315, https://doi.org/10.1016/j.epsl.2005.03.006.
- Ronov, A.B., 1982, The Earth's sedimentary shell (quantitative patterns of its structure, compositions, and evolution): The 20th VI Vernadskiy Lecture, March 12, 1978: International Geology Review, v. 24, no. 11, p. 1313–1363, https://doi .org/10.1080/00206818209451075.
- Royer, D.L., Berner, R.A., Montañez, I.P., Tabor, N.J., and Beerling, D.J., 2004, CO₂ as a primary driver of Phanerozoic climate: GSA Today, v. 14, no. 3, p. 4–10, https://doi.org/10.1130/1052-5173(2004) 014<4:CAAPDO>2.0.CO;2.
- Skelton, A., 2011, Flux rates for water and carbon during greenschist facies metamorphism: Geology, v. 39, p. 43–46, https://doi.org/10.1130/G31328.1.
- Stewart, E.M., and Ague, J.J., 2018, Infiltration-driven metamorphism, New England, USA: Regional CO₂ fluxes and implications for Devonian climate and extinctions: Earth and Planetary Science Letters, v. 489, p. 123–134, https://doi.org/10.1016/j.epsl.2018.02.028.
- Vidale, R.J., and Hewitt, D.A., 1973, "Mobile" components in the formation of calc-silicate bands: American Mineralogist: Journal of Earth and Planetary Materials, v. 58, no. 11–12, p. 991–997.
- West, A.J., Galy, A., and Bickle, M., 2005, Tectonic and climatic controls on silicate weathering: Earth and Planetary Science Letters, v. 235, no. 1–2, p. 211–228, https://doi.org/10.1016/j.epsl.2005.03.020.
- White, A.F., Schulz, M.S., Lowenstern, J.B., Vivit, D.V., and Bullen, T.D., 2005, The ubiquitous nature of accessory calcite in granitoid rocks: Implications for weathering, solute evolution, and petrogenesis: Geochimica et Cosmochimica Acta, v. 69, no. 6, p. 1455–1471, https://doi.org/10.1016/j.gca.2004.09.012.
- Whitley, S., Gertisser, R., Halama, R., Preece, K., Troll, V.R., and Deegan, F.M., 2019, Crustal CO₂ contribution to subduction zone degassing recorded through cale-silicate xenoliths in arc lavas: Scientific Reports, v. 9, article no. 8803, https://doi.org/10.1038/s41598-019-44929-2.
- Wong, K., Mason, E., Brune, S., East, M., Edmonds, M., and Zahirovic, S., 2019, Deep carbon cycling over the past 200 million years: A review of fluxes in different tectonic settings: Frontiers of Earth Science, v. 7, p. 1–22, https://doi.org/10.3389/feart.2019.00263.
- Zhang, S., FitzGerald, J.D., and Cox, S.F., 2000, Reaction-enhanced permeability during decarbonation of calcite + quartz → wollastonite + carbon dioxide: Geology, v. 28, p. 911–914, https://doi.org/10.1130/0091-7613(2000)28 <911:RPDDOC>2.0.CO;2.

Manuscript received 2 Dec. 2019 Revised manuscript received 11 Feb. 2020 Manuscript accepted 13 Feb. 2020